Flagellum/Stigma in Euglena gracilis

Subjects: Plant Sciences | Microbiology

Contributor: Kazunari Ozasa

Cell division of unicellular microalgae is a fascinating process of proliferation, at which whole organelles are regenerated and distributed to two new lives. We performed dynamic live cell imaging of Euglena gracilis using optical microscopy to elucidate the mechanisms involved in the regulation of the eyespot and flagellum during cell division and distribution of the organelles into the two daughter cells. Single cells of the wild type (WT) and colorless SM-ZK cells were confined in a microfluidic device, and the appearance of the eyespot (stigma) and emergent flagellum was tracked in sequential video-recorded images obtained by automatic cell tracking and focusing. We examined 12 SM-ZK and 10 WT cells and deduced that the eyespot diminished in size and disappeared at an early stage of cell division and remained undetected for 26–97 min (62 min on average, 22 min in deviation). Subsequently, two small eyespots appeared and were distributed into the two daughter cells. Additionally, the emergent flagellum gradually shortened to zero-length, and two flagella emerged from the anterior ends of the daughter cells. Our observation revealed that the eyespot and flagellum of E. gracilis are degraded once in the cell division, and the carotenoids in the eyespot are also decomposed. Subsequently, the two eyespots/flagella are regenerated for distribution into daughter cells. As a logical conclusion, the two daughter cells generated from a single cell division possess the equivalent organelles and each E. gracilis cell has eternal or non-finite life span. The two newly regenerated eyespot and flagellum grow at different rates and mature at different timings in the two daughter cells, resulting in diverse cell characteristics in E. gracilis.

microfluidic devices | automatic tracking system | eyespot | stigma | flagellum | SM-ZK | Euglena gracilis

1. Introduction

Cell division is a complex and fascinating process, and prompts researchers to investigate the detailed mechanisms of the process, especially the sequential changes occurring in chromosomes during division. The chromosomes in the nucleus replicate, separate into sister chromatids via the spindle and centrosomes, which results in two new nuclei. The sequential process of nucleus replication has been intensively investigated using optical/electron microscopy and has been elucidated in several eukaryote species. Other self-replicating multiple organelles such as lysosomes, ribosomes, plastids, and mitochondria have also been reported to be equally distributed into two daughter cells during cell division.

Numerous unicellular microbes with nuclei, including yeasts and microalgae, multiply solely via cell division. Some of these microbes possess single organelles, other than the nucleus. For example, the motile microalgae *Euglena*

gracilis has an emergent flagellum [1][2] and eyespot (or stigma) [1][3] in each cell, which constitutes single organelle. A simple but essential question arises as to how a single organelle is distributed into two daughter cells during cell division. Two simple possibilities can be conceived: one is that the single organelle is divided into two, and the other is that the original organelle is retained in one daughter cell and a new one is produced for the other daughter cell. It is essential to determine whether one of the two daughter cells receives the organelle from the parental cell as it would affect the life span of the cell. The life span of the cells may be considered “eternal” if both the daughter cells receive newly generated organelles and may be considered “finite” if one of the daughter cells contained the parental organelle and exhibits a shorter life span. The limitation of replicative life span has been reported for individual yeast cells [4], where the mother cell produces daughter cells through bud formation. In this case, only one daughter cell is generated at a time, and the process is relatively easy to track [5]. In contrast, tracking the cell division of *E. gracilis* is challenging. Live imaging at a high magnification is required to track organelles within the cell during cell division because the cells swim as fast as 200 μm/s or more, frequently change their shape, and exhibit euglenoid movements [1][6]. Confinement and fixation of a live cell in between two cover glasses is cumbersome as the cells escape from the observation area with euglenoid movements or are damaged severely by sandwiching pressure from the two glasses.

Non live cell imaging at a high magnification is relatively easier than dynamic live cell imaging and has been extensively carried out using electron microscopy. Walne and Arnott reported the comparative ultrastructure and possible function of eyespots in *E. granulata* and *Chlamydomonas eugametos* [7]. The authors stated that the eyespot granules develop by fusion of smaller granules. Their observations, however, provided only preliminary hints as to how the eyespot develops, to say nothing of the problem of how it replicates during cell division. Osafune and Schiff analyzed the stigma and flagellar swelling in relation to light and carotenoids using transmission electron microscopy [8]. The embedded *E. gracilis* cells were embedded in resin, sectioned, and stained before visualization. They observed that light is required to organize colored carotenoids into the spheres of stigma. Morel-Laurens et al. reported the effects of cell division on the stigma of *Chlamydomonas reinhardtii* and concluded that every daughter cell inherits a portion of the stigma of the maternal cell [9]. However, the mechanisms of stigma division/generation during cell division have not been clarified. Moreover, the mode of cell division differs considerably between *C. reinhardtii* [10] and *E. gracilis* [1].

In the present study, we performed dynamic live cell imaging of *E. gracilis* cell division using optical microscopy. Long-term tracking of a single moving cell was achieved by employing automatic XY-stage control, auto focusing of the microscope, and microfluidic devices for cell confinement. Cell division was recorded on video, and the appearance of the eyespot and the emergent flagellum (extended part out of the anterior of the cell body) was tracked in sequential images extracted from the video. We observed that the eyespot shrank and disappeared at the early stages of cell division. The emergent flagellum was retracted and disappeared before the start of nucleus segmentation. The eyespot remained undetected for approximately 30 min or more, and subsequently two small eyespots appeared and were distributed into two daughter cells. The flagellum was gradually protruded from the anterior portion of each daughter cell after the start of cell cleavage. Our observation revealed that the eyespot of *E. gracilis* is degraded/discarded once during cell division, or at least the carotenoids in the eyespot are extracted/decomposed. The two eyespots are newly reproduced for distribution to the daughter cells.

We also investigated the motility of parental and daughter cells and observed a relatively large difference (an average 18 min in 26 observed cells) in swimming initiation times among the daughter cells after cell division. The results imply that the two daughter cells develop their organelles at different rates, although they each possess each newly formed equivalent eyespot and flagellum.

2. Development and Findings

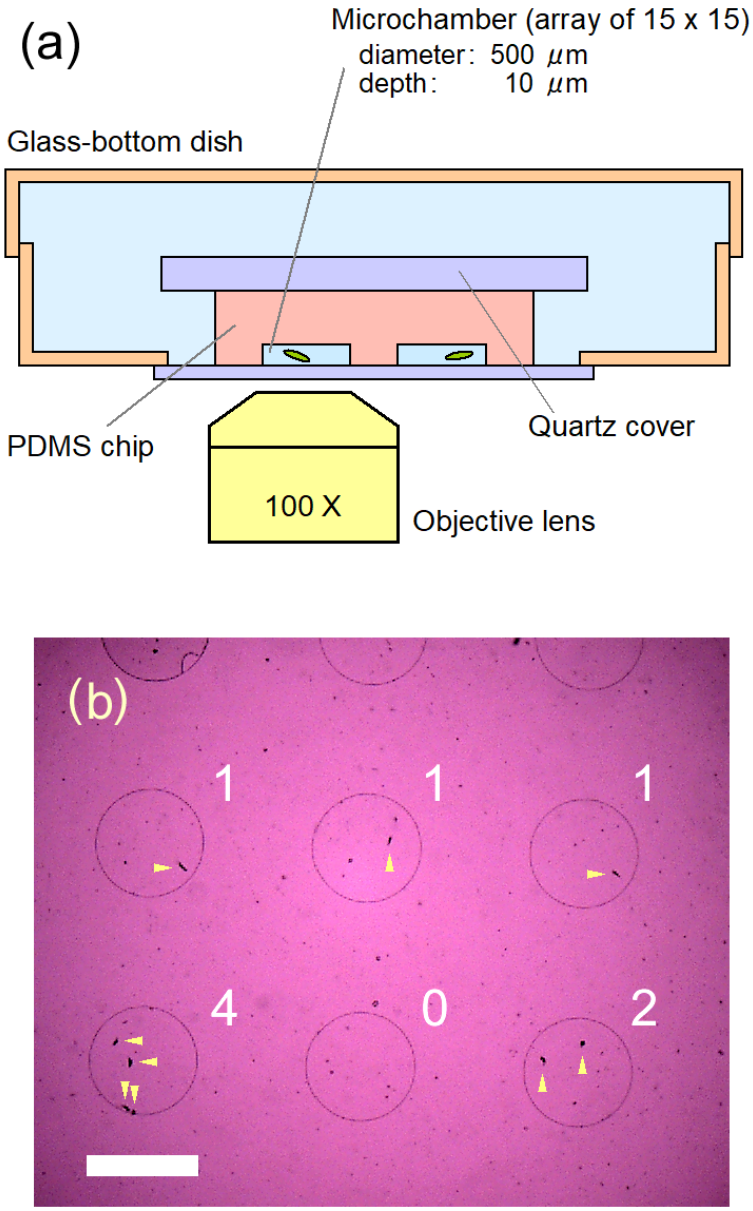

Figure 1. (**a**) Schematic drawing (cross-section, not in scale) of the microfluidic device used in this study. Some of microchambers held a single cell inside, by pressing down the soft porous PDMS chip onto the cell culture solution placed on the glass of the dish. The glass-bottom dish was then filled with pure water to prevent the microchambers from drying. The cells in the closed microchambers can survive three days or more. (**b**) A representative image of cells in confinement in our microfluidic device, observed with an objective lens of 4X.

Numbers in the figure show the number of cells confined in each microchamber, and arrows indicate the cells. Scale bar, 500 μm.

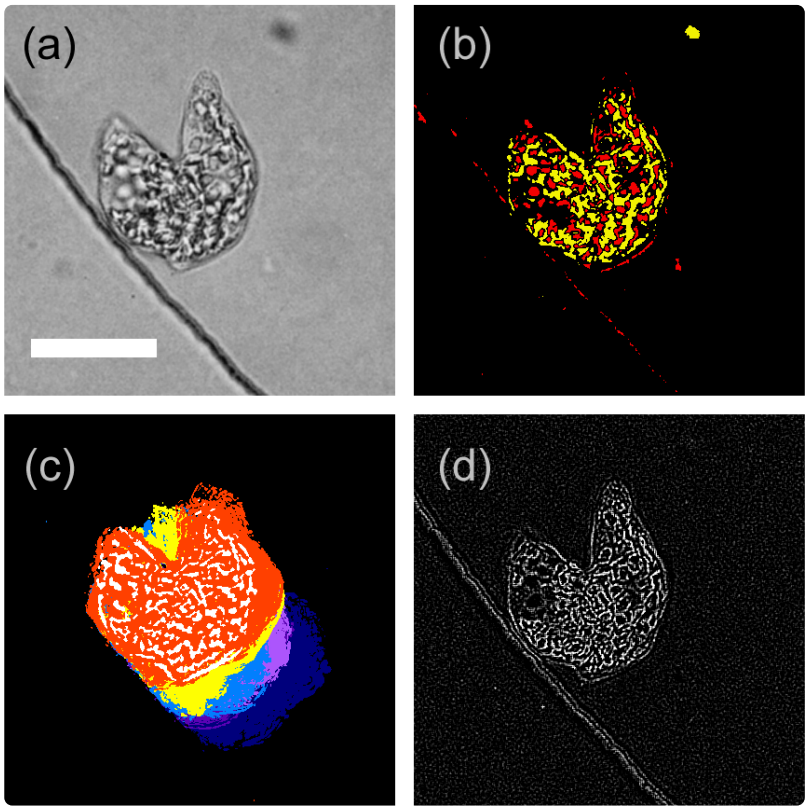

Figure 2. Examples of image processing for cell tracking, wherein a cell in the later stage of cell division at the edge line of circular microchamber was processed. (**a**) Captured image; obtained by 3 × 3 mean filtering with gray scaling. (**b**) Contrast image; obtained by thresholding brightness deviated from whole area average, i.e., the brighter part is colored in red, whereas the darker part is colored in yellow. (**c**) Trace image; obtained by time differential (frame-by-frame differential for each pixel) of the captured image, with further processing of binarization and integration for 20 frames (5.3 s). Five trace images were superimposed with different colors for effective visualization. (**d**) Focusing image; obtained by the spatial derivative for 3 × 3 pixels on the captured image. Scale bar, 20 μm.

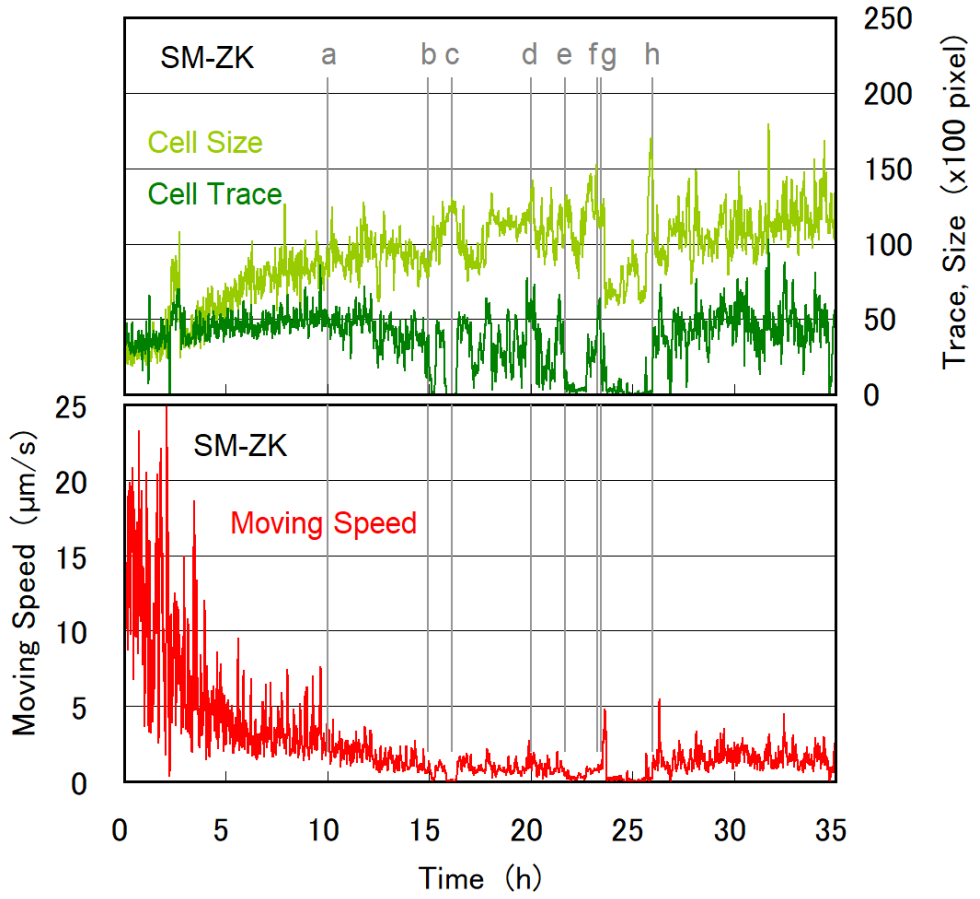

Figure 3. Temporal evolution of moving speed (velocity), cell size, and trace value obtained during the time course of cell division for an SM-ZK cell. Moving speed was calculated from XY-stage movement and the center of the gravity of the contrast image (e.g., **Figure 2**b). Cell size was obtained by counting red/yellow pixels in each contrast image (e.g., **Figure 2**b). The cell size represents the quasi-2D (10 μm thick) volume of the cell, assuming that cell height is at a uniform height of 10 μm. Trace value was obtained by estimating the non-zero pixels (white and red) in the trace image (e.g., **Figure 2**c). The trace value represents the momentum of cell movement and activity inside the cell. When the cell stops moving, the moving speed drops to zero, whereas the trace value may not become zero if the organelles move inside the cell. All of three values in **Figure 3** were time-averaged for 2 min. The contrast and trace images for (a) to (h), and video-recorded images are given in **Figure 4** and **Figure 5**, respectively.

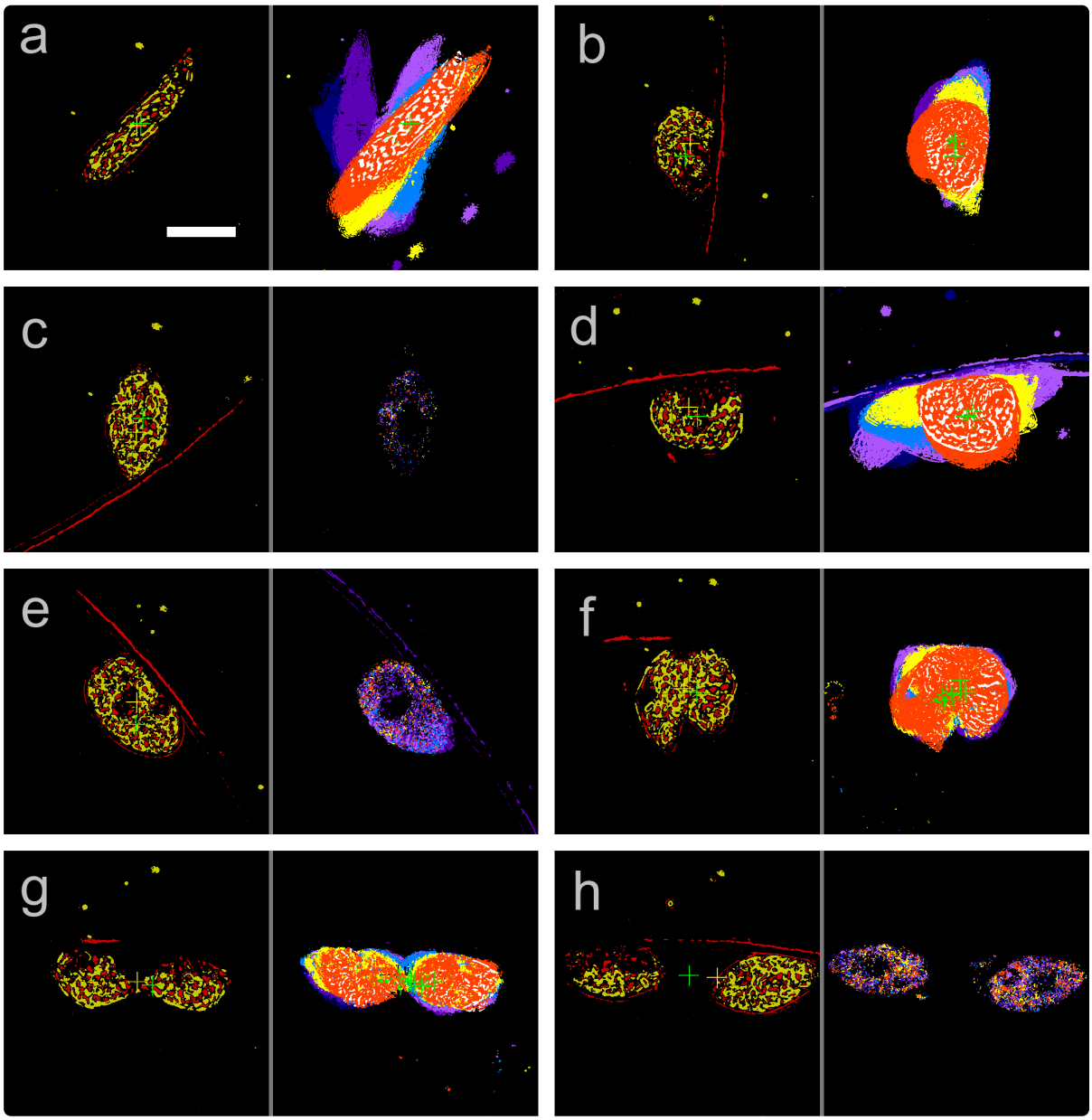

Figure 4. Contrast (**left**) and trace image (**right**) observed at (**a**) 10.0 h, (**b**) 15.0 h, (**c**) 16.1 h, (**d**) 20.0 h, (**e**) 21.7 h, (**f**) 23.3 h, (**g**) 23.5 h, and (**h**) 26.0 h. The time point of each image is given in **Figure 3** as vertical lines. Cross marks in the images are the center of gravity of non-zero pixels for the purpose of XY-stage control. Scale bar, 20 μm.

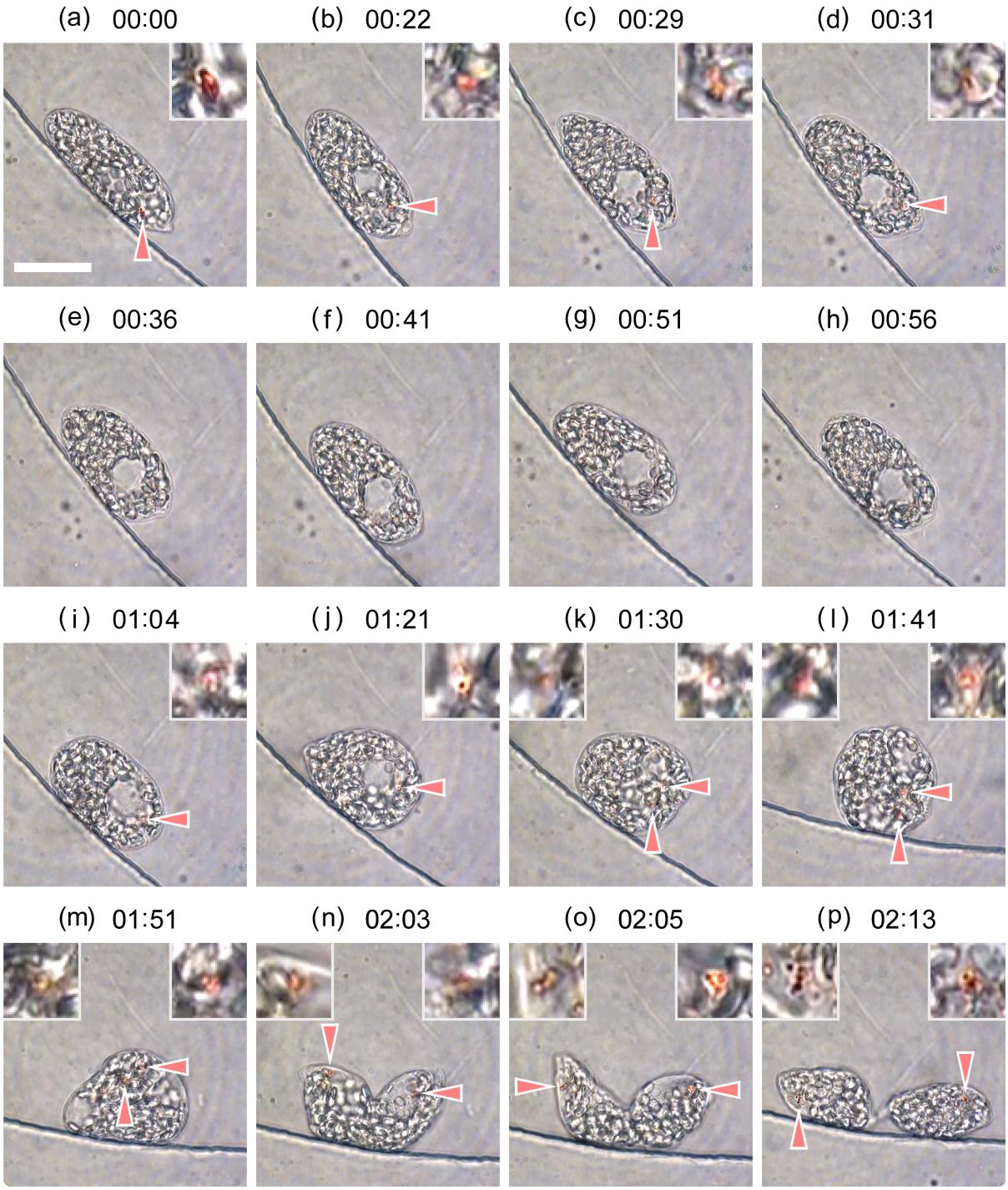

Figure 5. Images extracted from the video recording of the experiment depicted in **Figure 3**. (**a**) 21.24 h, (**b**) 21.60 h, (**c**) 21.72 h, (**d**) 21.75 h, (**e**) 21.83 h, (**f**) 21.92 h, (**g**) 22.08 h, (**h**) 22.17 h, (**i**) 22.30 h, (**j**) 22.58 h, (**k**) 22.73 h, (**l**) 22.92 h, (**m**) 23.08 h, (**n**) 23.28 h, (**o**) 23.32 h, and (**p**) 23.46 h. Time index given in the figure is shifted as reference; 00:00 (hh:mm) corresponds to 21.24 h in **Figure 3**. The eyespot indicated by arrow is enlarged by four times in the inset. Scale bar, 20 μm. Dynamic evolution of cell division is provided in the supplementary movie S3.

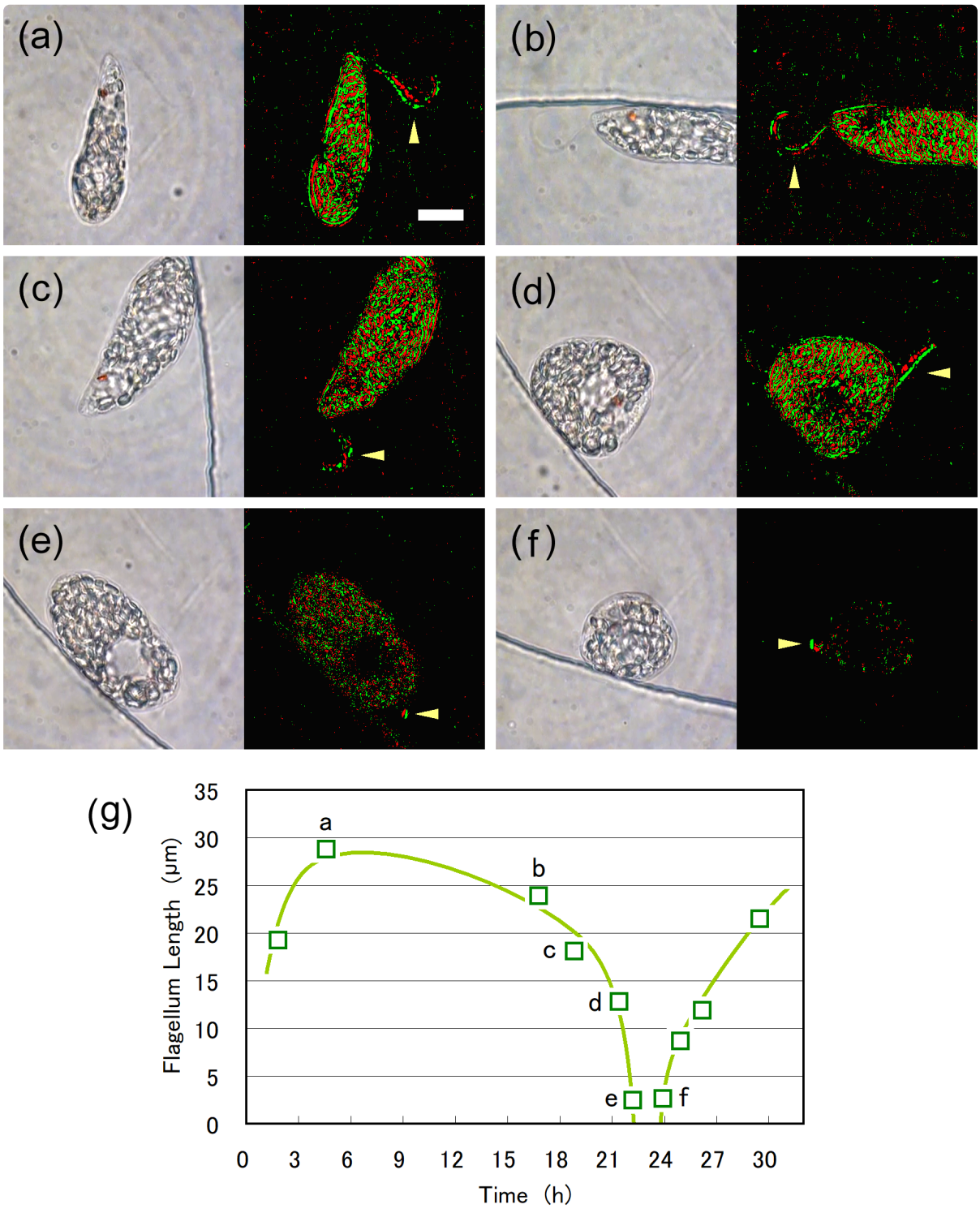

Figure 6. Shortening of the emergent flagellum, as seen in the images extracted from the video recording (**left** panels) and enhanced images (**right** panels) of the **Figure 5** case. Enhanced images were obtained with differentiation and binarization of two images at 61 ms intervals. The length of the emergent flagellum was (**a**) 29 μm at 4.57 h, (**b**) 24 μm at 16.78 h, (**c**) 18 μm at 18.83 h, (**d**) 13 μm at 21.41 h, (**e**) 2.5 μm at 22.18 h. (**f**) After the cell division, the emergent flagellum (2.6 μm in length) was first observed for one of the daughter cells at 23.91 h. Scale bar, 10 μm. (**g**) Temporal change in flagellum length. The graphical line is provided to indicate the trend.

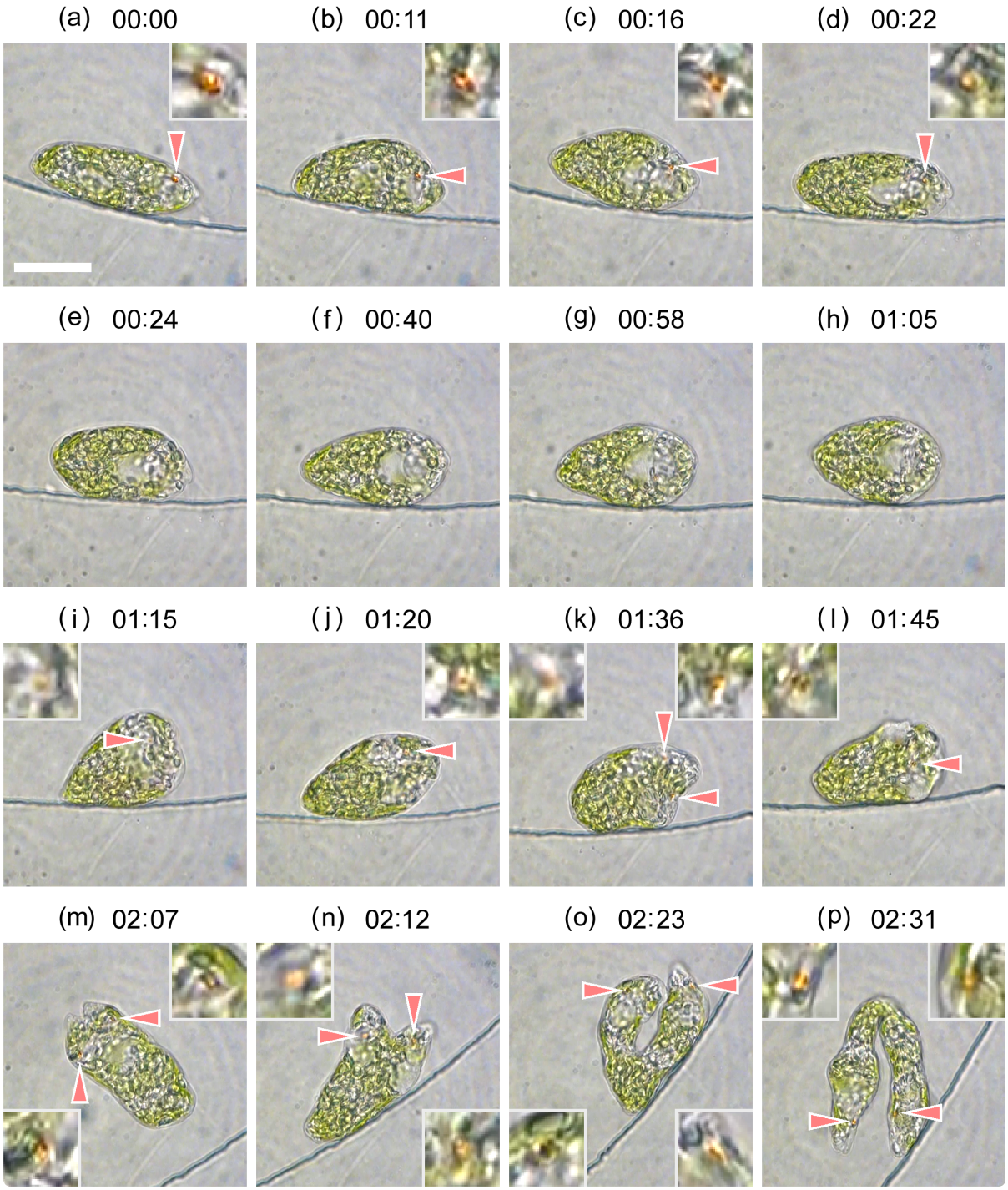

Figure 7. Images extracted from the video recording of the experiment depicted in Figure S1. (**a**) 17.52 h, (**b**) 17.70 h, (**c**) 17.79 h, (**d**) 17.89 h, (**e**) 17.92 h, (**f**) 18.19 h, (**g**) 18.49 h, (**h**) 18.60 h, (**i**) 18.77 h, (**j**) 18.85 h, (**k**) 19.12 h, (**l**) 19.27 h, (**m**) 19.64 h, (**n**) 19.72 h, (**o**) 19.90 h, and (**p**) 20.04 h. Time index given in the figure is shifted as a reference; 00:00 (hh:mm) corresponds to 17.52 h in Figure S1. The eyespot indicated by arrow is enlarged by four times in the inset. Scale bar, 20 μm. Dynamic evolution of cell division is provided in the supplementary movie S4.

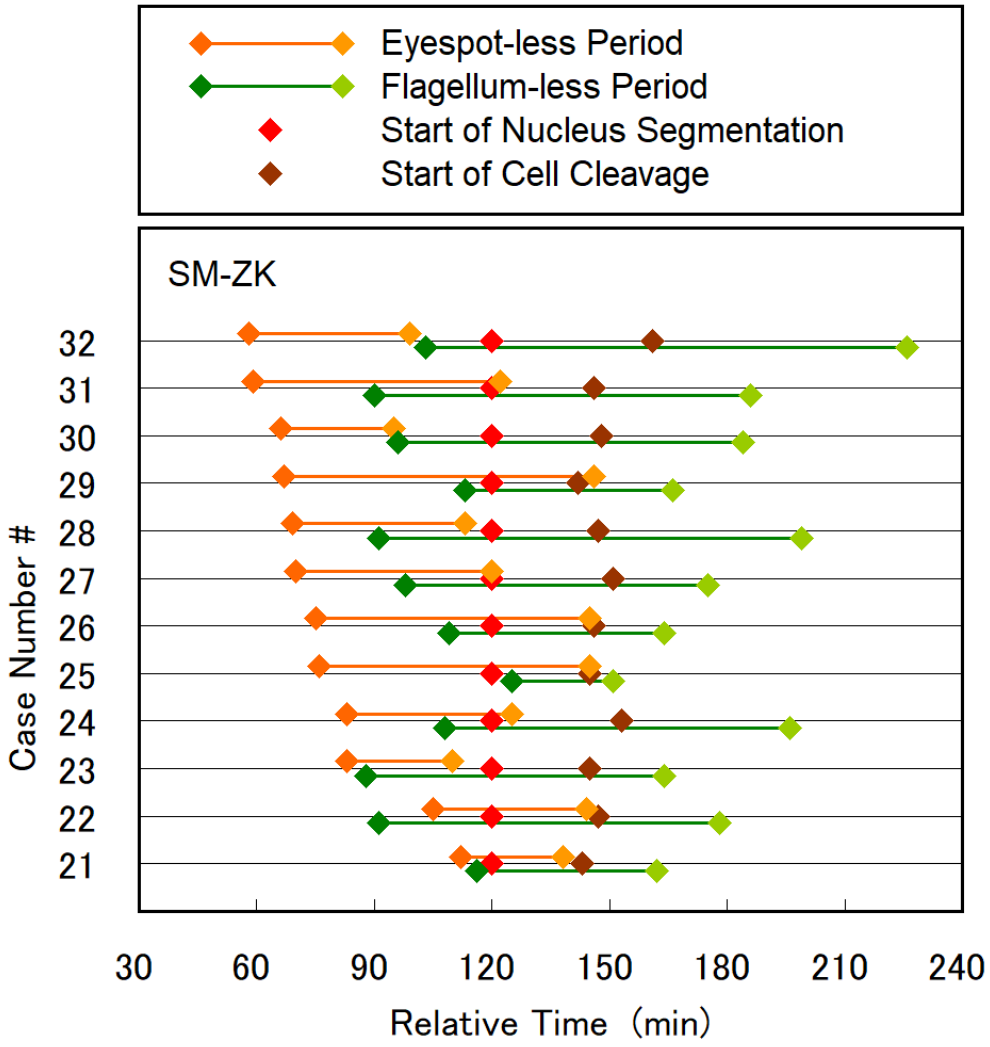

Figure 8. The period of disappearance of the eyespot and flagellum plotted for 12 SM-ZK cells, together with the initiation time of nucleus segmentation and cell cleavage. In the plot, the initiation time of nucleus segmentation was used as the standard timing (120 min). Case number was sorted by the time of eyespot disappearance (earlier to later). The case #30 corresponds to **Figure 3**, **Figure 5** and **Figure 6**, and Movie S3. See Figure S5 for WT cells.

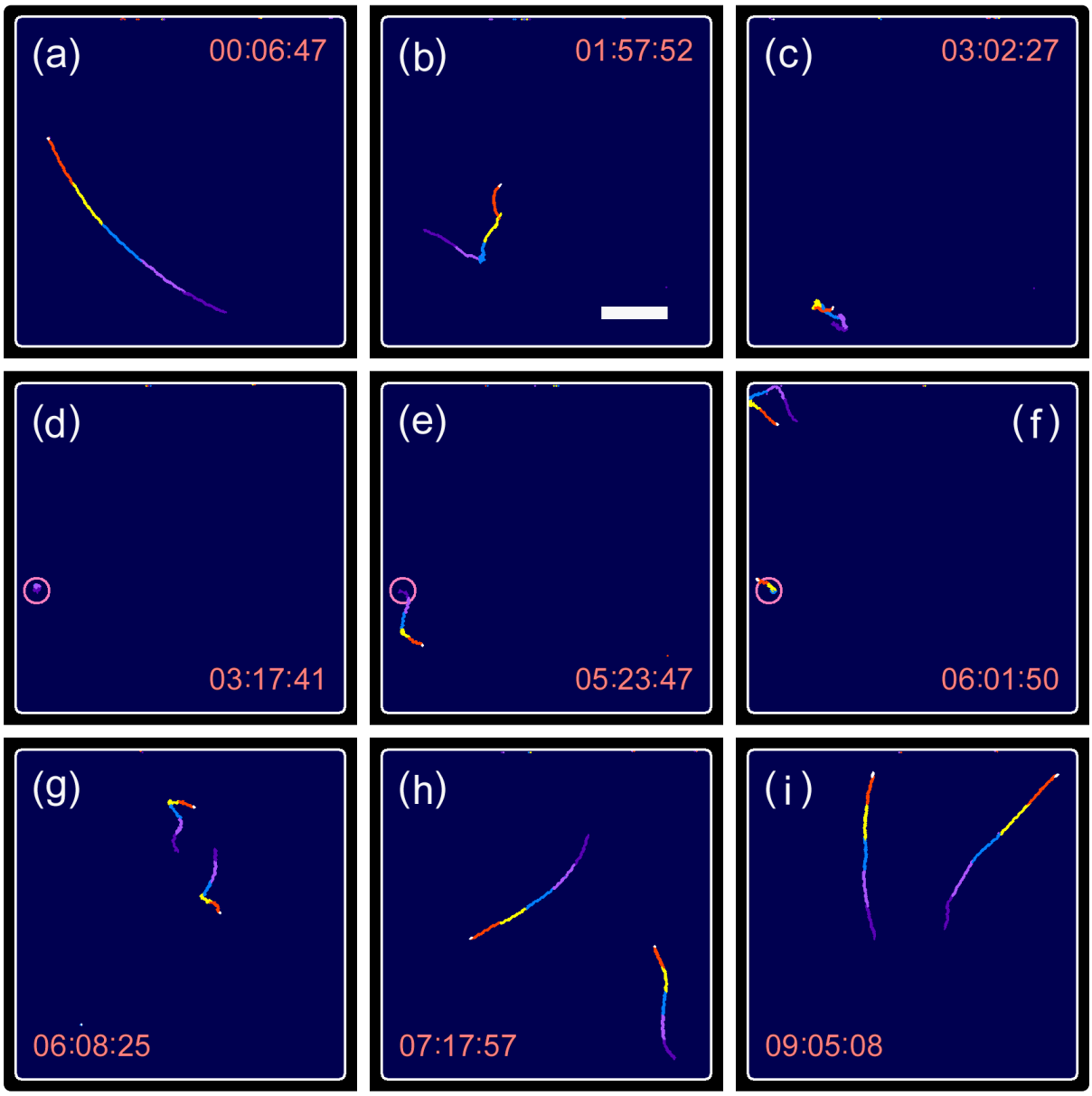

Figure 9. Swimming traces observed in a long-term millimeter-scale observation, including the period of cell division. (**a**–**d**) Movements of the parental cell, (**e**–**i**) movements of the daughter cells. In the images shown in (**a**–**i**), the traces obtained for the last 12.3 s (5 frames × 2.47 s/frame) were superimposed with different colors for visualization. Circles in (**d**–**f**) show the location where the cell division occurred. Refer to supplementary movie S6 for visualizing the entire process. Time index in the panels is indicated by hh:mm:ss. Scale bar, 500 μm.

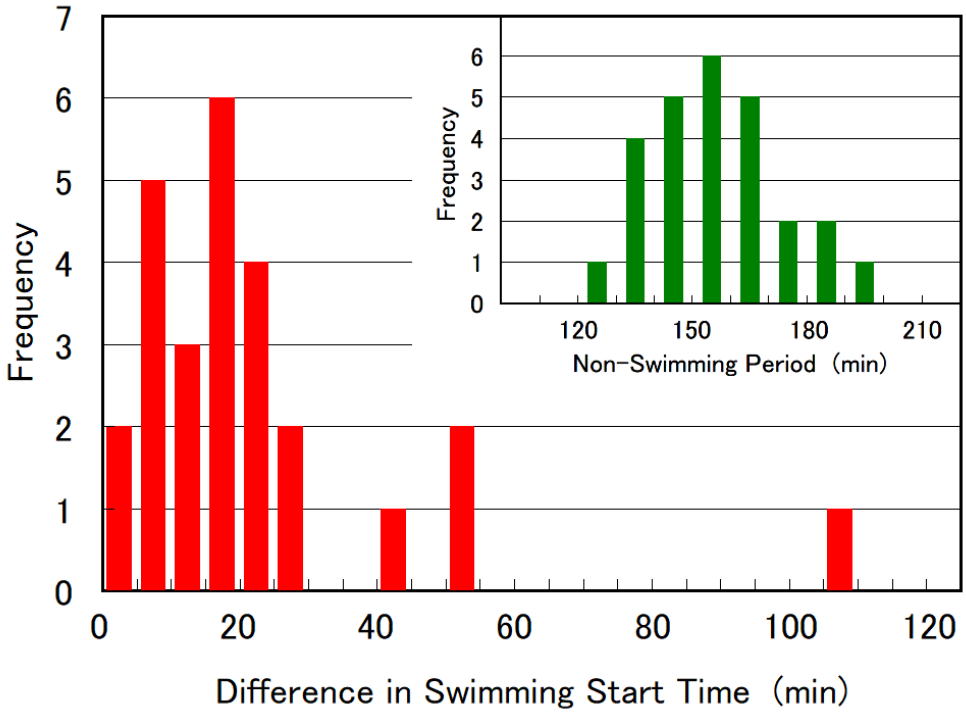

Figure 10. Histogram of the duration of cell division (non-swimming period) and difference in swimming start time between two daughter cells, based on data obtained from 26 individual SM-ZK cell divisions. The average cell division duration and difference in swimming start time was 157 and 38 min, respectively.

Although there are several studies on the cell division of *E. gracilis*, a majority of them focus on nucleus segmentation with a few describing eyespot behavior. Buetow reviewed the morphology and ultrastructure of *Euglena* [1] and reported that the stigma of *E. gracilis* is composed of many spherical granules (diameter of 100–300 nm), which are present in the cytoplasm in a loosely packed group [11][12]. The review also pointed out that the eyespot is a functionally specialized organelle, and that it is self-reproducing and occupies a defined portion of the cytoplasm. Leedale analyzed the mitotic cycle in live *E. gracilis* cells under an optical microscope, and showed that the locomotor apparatus (flagella, photoreceptor, and eyespot) replicates and the reservoir divides during early-to-late metaphase succession [13]. Hall and Jahn [14][15], and also Gojdics separately [16], reported that eyespot breaks up into its component granules during cell division at the stage of flagellum duplication or nucleus migration, with optical microscopy, although no evidential image showing eyespot break up was presented in their reports. Gillott and Triemer reported on the ultrastructure of *E. gracilis* at different stages of mitosis from preprophase to telophase, as observed under an electron microscope [17]. The only remark on the flagellum or eyespot found in the literature was that four non-emergent flagellar cross-sections were observed in a cell at prophase. Based on electron micrographs, Kivic and Vesk revealed that the eyespot replicated after nuclear division and segregated to opposite sides of the reservoir at about the same time as the flagella duplicated [18][19]. These observations and findings were, however, rather fragmented and non-qualitative, and observed in fewer cases. The dynamic live cell

imaging of *E. gracilis* cell division in the present study will offer insight into the replication processes of the eyespot and flagellum, as well as the mechanisms required for their reproduction.

Dynamic live cell imaging of cell division revealed that the eyespot of *E. gracilis* is removed/discarded once during cell division by a gradual shrinking process, or possibly the carotenoids in the eyespot are extracted/decomposed. We have not observed the break up of eyespot into a number of small globules in our dynamic live cell imaging of cell division, as suggested by the former literature [14][15][16]. On the other hand, Kato et al. reported that their genetically modified (Eg*crtB*-suppressed) colorless strain of *E. gracilis* had no obvious red eyespot but still possessed empty eyespot globules [20]. The report implies that the eyespot reproduction proceeds in two steps; the membranes of eyespot globules are reproduced, and then carotenoids accumulate into the globules. Figure S7a shows an example before the reappearance of the new distinctively discernible eyespot (after nucleus segmentation and before cell cleavage), in which a reddish brown hazy region can be seen between the two nuclei. This may present newly synthesized carotenoids, which will eventually be loaded into the eyespot globules.

The shortening of the emergent flagellum of *E. gracilis* is also the key for motility during cell division, i.e., the cell cannot swim due to the lack of emergent flagellum. The remaining issue in the flagellum shortening is whether the flagellum is decomposed from its outer end point or is retracted inside the reservoir from the backend. During the shortening process, a white dim spot was often observed at the outer end point of the flagellum (as shown in Figure S7b) even for extremely short flagellum of almost zero length. Although the origin of the white spot has not been identified, our observation suggests that the flagellum is retracted inside the reservoir, whereas the outer end point remains unchanged. The retraction of emergent flagellum during cell division has been also reported for *C. reinhardtii* [21].

The reason why *E. gracilis* degrades the eyespot and flagellum and regenerates them (instead of generating a new organelle and distributing new and old ones into two daughter cells) still remains enigmatic. We consider that the organellar decomposition/reproduction function of the organism is more basic and advantageous than that of division and distribution. Degradation of organelles is a basic function of cells and is required for the removal of unnecessary and defective cytosolic components. Regeneration of organelles is also frequently observed in microbes, as evidenced by the observation that *E. gracilis* cells regenerate their flagella once it is lost by external stimuli [22][23]. Beech et al. reviewed instances of flagellum duplication inside the basal body of algal flagellates, which included observations of flagellum shortening (*Epipyxis*) or complete retraction (*Chlamydomonas*, *Pleurochrysis*) during mitosis [24].

Our observation revealed that each of the two daughter cells of *E. gracilis* possess a newly replicated eyespot and emergent flagellum, and therefore the life span of *E. gracilis* may be “logically eternal.” At the same time, during the process of cell division shown in **Figure 5**, the two new eyespots were not generated simultaneously. One eyespot appeared approximately 25 min before the appearance of the second one (**Figure 5**i,k). Additionally, the two daughter cells seemed to grow at different rates after cell division, as evidenced by a relatively large difference in swimming start time (18 min on average, **Figure 10**). These observations suggested that the two newly regenerated eyespot and flagellum may grow at different rates and mature at different timings, possibly due to

unequal distribution of cytoplasm or stored nutrients in the two daughter cells during cell division. These differences produce diverse cellular characteristics of *E. gracilis*, such as in their motile behavior of gravitaxis [25], chemotaxis [26], and phototaxis [27][28][29]. Further investigation on cell division and maturity is required to explain this phenomenon in *E. gracilis* and other algal flagellates.

WT and SM-ZK cells contain a number of large paramylon granules, which tend to hinder the detection of the eyespot and detailed tracking of the shrinking eyespot. Upon suppression of paramylon production in SM-ZK cells using RNA interference or genetic modification, the eyespot reproduction process can be elucidated in detail using optical microscopy. The carotenoid specie present in the eyespot globules has been identified by Tamaki et al. as zeaxanthin [30]. Upon realization of fluorochrome-labeling of zeaxanthin molecules, fluorescence microscopy may be employed to track fluorochrome-labeled zeaxanthin molecules and analyze the replication process. Advanced laser processing method, such as eyespot destruction by focused femto-second laser pulses on live *E. gracilis* cells [31], is also a promising approach to investigate eyespot self-reproduction. A mutant *Euglena* strain containing plastids but no eyespot may be generated when eyespot regeneration is eliminated by advanced laser processing.

3. Conclusions

Our dynamic live cell imaging for 12 SM-ZK cells and 10 WT cells revealed the following. (1) The eyespot of *E. gracilis* was degraded once during cell division, or the carotenoids in the eyespot were decomposed. This process occurs predominantly 0.5–1.0 h prior to nucleus segmentation. (2) Two eyespots are gradually formed after ca. 0.5–1.5 h of its absence, and 0–0.5 h before the initiation of cell cleavage. (3) The emergent flagellum is retracted to zero-length 0–0.5 h before nucleus segmentation. (4) Two flagella gradually emerge 0.5–1.0 h after the initiation of cell cleavage (1.0–2.0 h of absence). (5) The newly regenerated eyespot and flagellum may grow and mature at different rates in the two daughter cells. Based on our microscopic observations, it is reasonable to assume that the two daughter cells are identical in terms of organelle age. These results also do not refute the hypothesis that the life span of *E. gracilis* may be “logically eternal,” although further studies are required to confirm it. The dynamic live cell imaging technique demonstrated in this study is an efficient approach to investigate organelle regeneration in unicellular microbes, especially on genetically modified strains of *E. gracilis* and other microalgae.

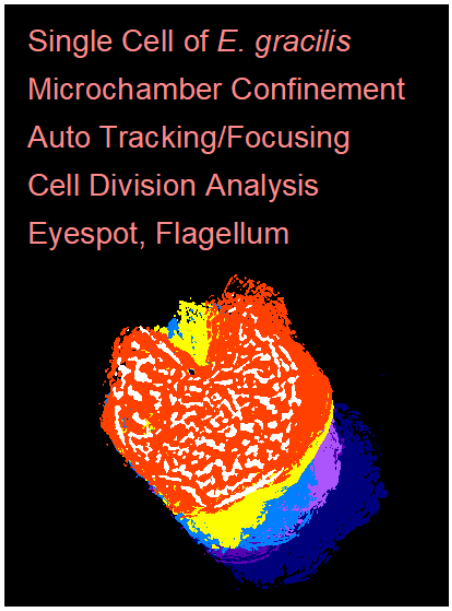

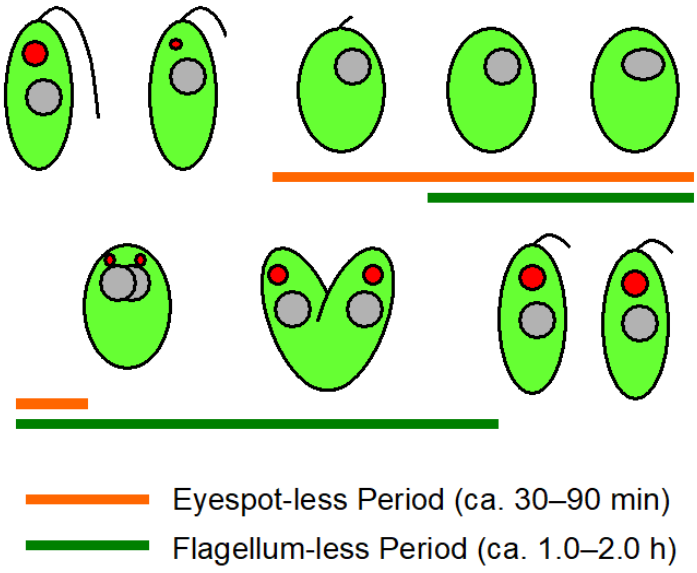

References

1. D. E. Buetow, The biology of Euglena, Vol. III: Physiology, New York, Academic Press (1982).
2. P. Gualtieri, K. Barsanti, V. Passarelli, F. Verni, G. Rosati, A look into the reservoir of Euglena gracilis: SEM investigations of the flagellar apparatus, Micron Microscopica Acta, 21, 131-138 (1990).
3. T. W. James, F. Crescitelli, E. R. Loew, W. N. McFarland, The eyespot of euglena gracilis: a microspectrophotometric study, Vision Res., 32, 1583-1591 (1992).
4. R. K. Mortimer, J. R. Johnston, Life span of individual yeast cells, Nature, 183, 1751-1752 (1959).
5. K. K. Steffen, B. K. Kennedy, M. Kaeberlein, Measuring replicative life span in the budding yeast, J. Vis. Exp., 28, e1209 (2009).
6. J. M. Murray, Control of cell shape by calcium in the Euglenophyceae, J. Cell Sci., 49, 99-117 (1981).
7. P. L. Walne and H. J. Arnott, The comparative ultrastructure and possible function of eyespots: Euglena granulata and Chlamydomonas eugametos, Planta, 77, 325-353 (1967).
8. T. Osafune and J. A. Schiff, Stigma and flagellar swelling in relation to light and carotenoids in Euglena gracilis var. bacillaris, J. Ultrastruct. Res., 73, 336-349 (1980).
9. N. M. L. Morel-Laurens, D. J. Bird, Effects of cell division on the stigma of wild-type and an eyeless mutant of Chlamydomonas, J. Ultrastruct. Res., 87, 46-61 (1984).
10. F. R. Cross, J. G. Umen, The Chlamydomonas cell cycle, Plant J., 82, 370-392 (2015).

11. J. J. Wolken, E. Shin, Photomotion in Euglena gracilis I. Photokinesis II. Phototaxis, Eukaryotic Microbiol., 5, 39-46 (1958).
12. S. P. Gibbs, The fine structure of Euglena gracilis with special reference to the chloroplasts and pyrenoids, J. Ultrastruct. Res., 4, 127-148 (1960).
13. G. F. Leedale, The nucleus in Euglena, chap 5, in D. E. Buetow Ed., The biology of Euglena, Vol. I, New York, Academic Press (1968).
14. R. P. Hall, T. L. Jahn, On the comparative cytology of certain euglenoid flagellates and the systematic position of the families euglenidae stein and astasiidae butschli, Trans. Am. Micrscop. Soc., 48, 388-405 (1929).
15. R. P. Hall, T. L. Jahn, Dispersed stages of the stigma in euglena, Science, 69, 522 (1929).
16. M. Gojdics, The cell morphology and division of euglena deses ehrge, Trans. Am. Microscop. Soc., 53, 299-310 (1934).
17. M. A. Gillott, R. E. Triemer, The ultrastructure of cell division in Euglena gracilis, J. Cell Sci., 31, 25-35 (1978).
18. P. A. Kivic, M. Vesk, Structure and function of the euglenoid eyespot, J. Exper. Botany, 23, 1070-1075 (1972).
19. P. A. Kivic, M. Vesk, Structure and function in the euglenoid eyespot apparatus: the fine structure, and response to environmental changes, Planta, 105, 1-14 (1972).
20. S. Kato, K. Ozasa, M. Maeda, Y. Tanno, S. Tamaki, M. Higuchi-Takeuchi, K. Numata, Y. Kodama, M. Sato, K. Toyooka, T. Shinomura, Carotenoids are essential for light perception by the eyespot apparatus to initiate the phototactic movement of Euglena gracilis, Plant J., 101, 1091-1102 (2020).
21. T. Cavalier-Smith, Basal body and flagellar development during the vegetative cell cycle and the sexual cycle of Chlamydomonas Reinhardii, J. Cell Sci., 16, 529-556 (1974).
22. G. M. Habib, B. G. Bouck, Synthesis and mobilization of flagellar glycoprotein during regeneration in Euglena, J. Cell Biol., 93, 432-441 (1982).
23. H. Okuwa-Hayashi, H. Inui, J. Inagaki, M. Nakazawa, S. Ebara, T. Sakamoto, Y. Nakano, Effect of nicotinamide on the flagellar detachment and regeneration of Euglena, Vitamins (Japan), 93, 115-122 (2019).
24. P. L. Beech, K. Heimann, M. Melkonian, Development of the flagellar apparatus during the cell cycle in unicellular algae, Protoplasma, 164, 23-37 (1991).
25. K. Ozasa, H. Kang, S. Song, S. Kato, T. Shinomura, M. Maeda, Temporal Evolution of the Gravitaxis of Euglena gracilis from a Single Cell, Plants, 10, 1411 (2021).

26. K. Ozasa, J. Lee, S. Song, M. Hara, M. Maeda, Gas/liquid sensing via chemotaxis of Euglena cells confined in an isolated micro-aquarium, LabChip, 13, 4033-4039 (2013).
27. M. Iseki, S. Matsunaga, A. Murakami, K. Ohno, K. Shiga, K. Yoshida, M. Sugai, T. Takahashi, T. Hori, M. Watanabe, A blue-light activated adenylyl cyclase mediates photoavoidance in Euglena gracilis. Nature 415, 1047-1051 (2002).
28. K. Ozasa, J. Lee, S. Song, M. Maeda, Transient freezing behavior in photophobic responses of Euglena gracilis investigated in a microfluidic device, Plant Cell Physiol., 55, 1704-1712 (2014).
29. K. Ozasa, J. Won, S. Song, S. Tamaki, T. Ishikawa, M. Maeda, Temporal change of photophobic step-up responses of Euglena gracilis investigated through motion analysis. PLoS ONE, 12, e0172813 (2017).
30. S. Tamaki, Y. Tanno, S. Kato, K. Ozasa, M. Wakazaki, M. Sato, K. Toyooka, T. Maoka, T. Ishikawa, M. Maeda, T. Shinomura, Carotenoid accumulation in the eyespot apparatus required for phototaxis is independent of chloroplast development in Euglena gracilis, Plant Sci., 298, 110564 (2020).
31. A. Vogel, J. Noack, G. Huttmann, G. Paltauf, Mechanisms of femtosecond laser nanosurgery of cells and tissues, Appl. Phys. B, 81, 1015-1047 (2005).